

Antisite Domains in Double Perovskite Ferromagnets: Impact on Magnetotransport and Half-metallicity

VIVEKA NAND SINGH and PINAKI MAJUMDAR

Harish-Chandra Research Institute, Chhatnag Road, Jhusi, Allahabad 211019, India

PACS 75.47.Lx – Magnetic oxides
 PACS 75.47.Gk – Colossal magnetoresistance
 PACS 75.60.Ch – Domain walls and domain structure

Abstract. - Several double perovskite materials of the form $A_2BB'O_6$ exhibit high ferromagnetic T_c , and significant low field magnetoresistance. They are also a candidate source of spin polarized electrons. The potential usefulness of these materials is, however, frustrated by mislocation of the B and B' ions, which do not organise themselves in the ideal alternating structure. The result is a strong dependence of physical properties on preparative conditions, reducing the magnetization and destroying the half-metallicity. We provide the first results on the impact of *spatially correlated* antisite disorder, as observed experimentally, on the ferromagnetic double perovskites. The antisite domains suppress magnetism and half-metallicity, as expected, but lead to a dramatic enhancement of the low field magnetoresistance.

Double perovskite (DP) materials, of the form $A_2BB'O_6$, are of interest on account of their unusual magnetic and transport properties [1]. In particular, some double perovskites, *e.g.*, Sr_2FeMoO_6 , show high ferromagnetic T_c , $\sim 420K$, half-metallic behavior, and large low field magnetoresistance [2, 3]. Other double perovskites, *e.g.*, Sr_2FeWO_6 , are antiferromagnetic insulators [4], while some show unusual dielectric properties [5].

Usually one of the ions, B, say, is magnetic and the other (B') is non-magnetic. Magnetic ordering in these materials arises from a combination of strong electron-spin coupling on the B ion and electron delocalisation on the B-O-B' network [6–8]. The magnetic order, however, is also strongly affected by the *local ordering* of the B and B' ions [9–16]. A B-O-B arrangement, for example, favours antiferromagnetic locking of the two B moments rather than parallel alignment. Most real materials have some degree of such 'antisite disorder' (ASD) with mislocated B and B' ions. The promise of rich functionality in the DP's remains unfulfilled due to this inevitable B, B' mislocation.

Let us summarise the key observations on Sr_2FeMoO_6 (SFMO), the prototype DP, to establish the tasks for a theory of antisite disorder in these materials. (i) *Nature of defects:* there is clear evidence now that B-B' mislocations are not random but spatially correlated [17, 18]. While ASD suppresses long range structural order, electron microscopy [17] and XAFS [18] reveal that a high

degree of short range order survives. (ii) *Magnetism:* the ASD brings into play a B-B AF coupling, via B-O-B links, that makes neighbouring FM regions antiparallel. This reduces the bulk moment from $M_{max} \sim 4\mu_B$ expected in 'ordered' SFMO. The T_c is *not* significantly affected by ASD, till very large disorder. The magnetic effects of ASD are similar in both single crystals and polycrystals [2, 3, 10]. (iii) *Transport:* resistivity results are widely different between single crystals and polycrystals. Single crystals [3] show residual resistivity $\rho \sim 0.1m\Omega cm$, and metallic behaviour, $d\rho/dT > 0$. The magnetoresistance (MR) is weak, $< 10\%$ at low temperature at a field of 5 Tesla. Unfortunately, single crystal data with systematic variation of ASD is not available. Polycrystalline samples have been studied [10–14, 19] for a wide range of ASD *but* the transport in these materials is affected also by grain boundary (GB) resistance. The residual resistivity in these samples [10] range from $\sim 0.5m\Omega cm$ for low ASD ($M/M_{max} \sim 1.0$) to $\sim 10m\Omega cm$ at high ASD ($M/M_{max} \sim 0.5$). 'Ordered' polycrystals show $d\rho/dT > 0$, while the less ordered ones [10, 11] show $d\rho/dT < 0$. The MR can be large, $\sim 40\%$ at low temperature and 5 Tesla [11], and seems to be dominated by grain boundary effects [14, 19]. Some results indicate a decrease [11] in MR with increasing ASD, others show an increase [12]. The effects of antisite disorder and grain boundaries on MR have not been deconvolved yet.

In this paper we *build in* the correlated antisite disorder and study its impact on magnetism and *intrinsic transport* in the double perovskites. We ignore the effect of grain boundaries, admittedly important in polycrystals, but uncover a metal-insulator transition and large MR that can result from antisite disorder itself.

Our main results, based on large lattices in two dimensions (2D), are the following. (i) Correlated antisite disorder leads to structural antiphase boundaries (APB) that also act as magnetic domain walls (MDW) at low temperature. (ii) Growing ASD suppresses the saturation magnetisation, leaves the T_c mostly unaffected, but leads to a metal-insulator transition in the electronic ground state. (iii) The ‘insulating’ samples have huge low field MR at low temperature since domain rotation ‘unblocks’ conduction paths. (iv) The conduction spin polarisation roughly follows the core spin magnetisation in its disorder and temperature dependence. Overall, moderate ASD seems to be *beneficial*, since it enhances the MR without destroying the half-metallicity or suppressing the T_c .

Model and method. – The ASD arises from an annealing process, and is spatially correlated [17, 18] rather than random. Generating antisite disordered configurations that incorporate the detailed B, B’ chemistry and capture specific preparative conditions is difficult. However, one can model the inherent ordering tendency in the B, B’ system, and frustrate it via poor annealing to mimic the situation in the material. Using the structural motifs that emerge [20] we can then solve the coupled electronic-magnetic problem through a real space technique.

We use a binary variable η_i to encode information about atomic positions. We set $\eta_i = 1$ for B sites and $\eta_i = 0$ for B’ sites. In a non disordered DP the η_i will alternate along each axis. We will consider spatially correlated disordered configurations of η , discussed later, and for any specified $\{\eta\}$ background the electronic-magnetic model has the form:

$$\begin{aligned}
H = & \epsilon_B \sum_{i\sigma} \eta_i f_{i\sigma}^\dagger f_{i\sigma} + \epsilon_{B'} \sum_{i\sigma} (1 - \eta_i) m_{i\sigma}^\dagger m_{i\sigma} \\
& + H_{kin}\{\eta\} + J \sum_{i\alpha\beta} \eta_i \mathbf{S}_i \cdot f_{i\alpha}^\dagger \vec{\sigma}_{\alpha\beta} f_{i\beta} \\
& + J_{AF} \sum_{\langle i,j \rangle} \eta_i \eta_j \mathbf{S}_i \cdot \mathbf{S}_j - h \sum_i S_{iz} \quad (1)
\end{aligned}$$

Here f is the electron operator corresponding to the magnetic B site and m is that of the non-magnetic B’ site. ϵ_B and $\epsilon_{B'}$ are onsite energies, at the B and B’ sites respectively. $\epsilon_B - \epsilon_{B'}$ is a ‘charge transfer’ energy. H_{kin} is the electron hopping term: $-t_1 \sum_{\langle i,j \rangle \sigma} \eta_i \eta_j f_{i\sigma}^\dagger f_{j\sigma} - t_2 \sum_{\langle i,j \rangle \sigma} (1 - \eta_i)(1 - \eta_j) m_{i\sigma}^\dagger m_{j\sigma} - t_3 \sum_{\langle i,j \rangle \sigma} (\eta_i + \eta_j - 2\eta_i \eta_j)(f_{i\sigma}^\dagger m_{j\sigma} + h.c)$. The t ’s are all nearest neighbour hopping amplitudes, and for simplicity we set $t_1 = t_2 = t_3 = t$ here. \mathbf{S}_i is the core spin on the site \mathbf{R}_i , and $|\mathbf{S}_i| = 1$. J is the Hund’s coupling on the B sites, and we use $J/t \gg 1$. When the ‘up spin’ core levels are fully

filled, as for Fe in SFMO, the conduction electron is forced to be *antiparallel* to the core spin. We have used $J > 0$ to model this situation. For the present study we have set [21] the *effective* charge transfer energy $\epsilon_B - J/2 - \epsilon_{B'} = 0$.

If two magnetic atoms are on neighbouring sites, we also have to consider the *antiferromagnetic* (AF) coupling between them. Much of the physics of these materials arises from the competition between delocalisation driven ferromagnetic exchange and this B-B superexchange. We set $J_{AF} S^2/t = 0.08$, based on the T_N scale in SrFeO₃. h is an applied magnetic field in the \hat{z} direction

The model above treats the variables η_i as given. What governs the distribution of ionic positions $\{\eta_i\}$? The effective interaction between ions has a ‘direct’ component (Lennard-Jones, say) that we label V_{ion} . There is also the *indirect* interaction via the electronic-magnetic degrees of freedom in $H\{\eta_i\}$. The total Hamiltonian, including all degrees of freedom, would be: $H_{tot} = H\{\eta_i\} + V_{ion}\{\eta_i\}$. To obtain the effective interaction among the $\{\eta_i\}$ one should trace out the electronic and magnetic variables. So, the effective potential $V_{eff}\{\eta\}$ controlling the positional order is $V_{eff}\{\eta\} = -(1/\beta) \log \int \mathcal{D}\mathbf{S}_i Tr_{\{f,m\}} e^{-\beta H_{tot}}$. Unfortunately there is limited information about V_{ion} , and the trace is computationally demanding. Thankfully, the experiments themselves suggest a way ahead.

Firstly, the structural degrees of freedom ‘freeze’ at a temperature $T_{ord} \sim 1000\text{K} \gg T_c \sim 400\text{K}$, where T_c is the magnetic ordering temperature, so we need not bother about the ‘feedback’ of magnetic and electronic degrees of freedom on the $\{\eta_i\}$ ordering. Secondly, the tendency is to order into an alternating pattern, frustrated by short annealing. So, as a first attempt, we can try out a simple short range model with the same tendency. Concretely, we use a ‘lattice gas’ model $V_{eff}\{\eta\} = -V \sum_{\langle ij \rangle} \eta_i (1 - \eta_j)$ with $V > 0$ being a measure of the ordering tendency. The ground state in this model would correspond to $\eta = 1, 0, 1, 0, \dots$ along each axis, *i.e.*, B, B’, B, B’,... This approach tries to incorporate the effect of complex interactions between the A, B, B’ and O ions (as also the electrons) into a single parameter V .

We explored [20] the consequences of different annealing protocols on this model, to examine the consequences of imperfect annealing. The lattice gas model has a finite temperature transition in both 2D and 3D. We work in 2D since it allows access to large sizes and is easier to visualise.

One can variously characterise the B-B’ structures that emerge. We use the following simple indicators, to keep a close correspondence with the experimental work. (i) The fraction of B (or B’) atoms that are on the wrong sublattice, call this x , and the structural ‘order parameter’ $S = 1 - 2x$. (ii) The degree of short range order, characterised by the probability, p , of having nearest neighbour pairs that are B-B’. (iii) The correlation length ξ in these structures, computed from the width of the ordering peak.

For a given $\{\eta_i\}$ configuration we need to solve for the magnetic and electronic properties. Since the background

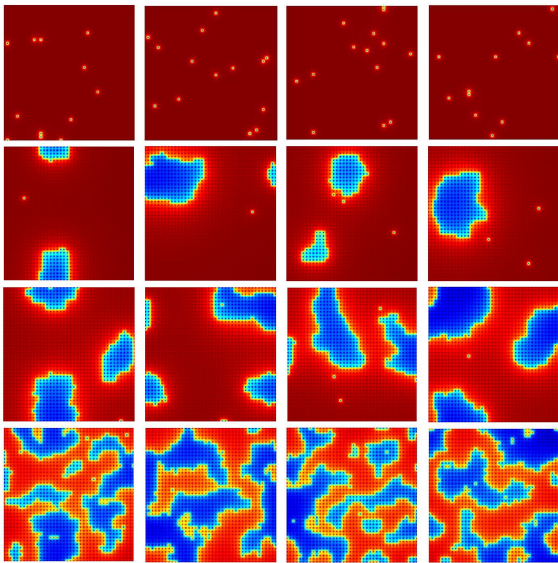


Fig. 1: Colour online: We show four families of antisite disordered configurations (top to bottom) generated via successively poorer annealing of the lattice gas model. We plot $(\eta_i - 1/2)e^{i\pi(x_i + y_i)}$. For a perfectly ordered structure $g(\mathbf{R}_i)$ is constant. The patterns along a row are different realisations of ASD within each family. The average structural order parameter (see text) has values $S = 0.98, 0.76, 0.50$ and 0.08 as we move from top to bottom. Lattice size 40×40 .

involves strong disorder, and the electron-spin coupling, J , is large, we use an exact diagonalization based Monte Carlo (ED-MC) technique. This uses the Metropolis algorithm where a spin update, $\mathbf{S}_i \rightarrow \mathbf{S}'_i$ is accepted or rejected depending on $\Delta E/k_B T$, where $\Delta E = E(\mathbf{S}'_i) - E(\mathbf{S}_i)$. In principle we should diagonalise the full system every time an update is attempted. The cost, for a large system, is prohibitive, so we employ a method [22] where we diagonalize a cluster Hamiltonian built around the update site.

Electronic properties are calculated after equilibration by diagonalizing the full system. The optical conductivity is calculated via the Kubo formulation. The ‘dc conductivity’ is the low frequency average [23], $\sigma_{dc} = (1/\Delta\omega) \int_0^{\Delta\omega} \sigma(\omega) d\omega$, where $\sigma(\omega)$ is thermal and disorder averaged, and $\Delta\omega \sim 0.05t$. Our ‘dc resistivity’ is the inverse of this σ_{dc} . The spin resolved density of states $D_\sigma(\omega)$ is calculated from the single particle Green’s function.

Earlier work. – The theoretical effort till now [15,16] has focused on *uncorrelated* antisite disorder, and quantified the impact of such ASD on magnetic properties. One of them [15] is based on a variational scheme in large 3D systems, and quantifies the doping and antisite concentration dependence of magnetic properties. The other [16] uses a classical spin model for magnetism, and studies the critical properties. These calculations set the reference for magnetic properties but have the obvious limitation that: (i) they use randomly located antisites, (ii) they do not clarify the electronic properties, and (iii) the estimate

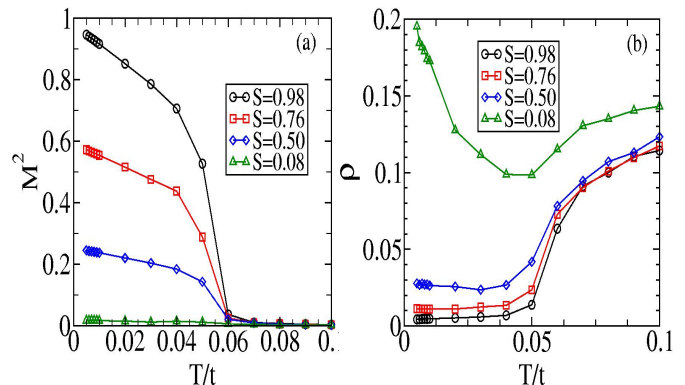


Fig. 2: Colour online: (a). The ferromagnetic peak in the structure factor, M^2 , where M is the magnetisation, for different degrees of antisite disorder. (b) The ‘d.c resistivity’, $\rho(T)$ for varying antisite disorder. Results are on a 40×40 lattice, averaged thermally and over 10 copies of disorder.

of localisation effects that arise from structural/magnetic domains, and the possible MR, remains unexplored.

Results. –

ASD configurations. The ASD configurations can be readily generated through a Monte Carlo on the lattice gas model. Below an ordering temperature $T_{ord} \sim 0.7V$ (in 2D) the model exhibits long range B-B’ order *provided one anneals long enough*. We quench the system from high temperature (random B, B’) to $T_{ann} < T_{ord}$, but deliberately anneal it for a short time, preventing equilibration. The details have been discussed [20] in an earlier paper. The four families we chose, see Fig.1, have a fraction of mislocated sites: $x = 0.01, 0.12, 0.25, 0.46$. The patterns, however, are strongly correlated. Even in the most disordered samples (lowest row in Fig.1) where the likelihood of any site being B or B’ is ~ 0.5 , if a site is B, say, there is a high likelihood that its neighbours will be B’ (and vice versa). Following recent experimental work [18], we calculate the probability p of having B-B’ nearest neighbours as a measure of short range correlation. In a perfectly ordered sample this would be 1 (the B, B’ alternate) while in a completely disordered sample this is 0.5. For an uncorrelated B, B’ distribution this is $p_{uncorr} = x^2 + (1-x)^2 = (1/2)(1+S^2)$. If we only knew S , these would lead to $p_{uncorr} = 0.98, 0.79, 0.63, 0.50$ for the x that we have used. The values that actually emerge from analysing our correlated patterns, are $p_{corr} \sim 0.98, 0.97, 0.95, 0.86$. Even the most disordered samples have a high degree of short range order. A Lorentzian fit to the B-B’ structure factor, of the form $S_{BB'}(\mathbf{q}) \sim \xi^{-1}/((q_x - \pi)^2 + (q_y - \pi)^2 + \xi^{-2})$, yields $\xi \sim 6.6, 5.9, 4.8, 3.6$.

Disorder dependence at $T = 0$. Let us examine the effect of the ASD on the magnetic properties. Suppose the fraction of mislocated B, B’ sites is x , and the structure is organised into domains such that the ratio of ‘perimeter’

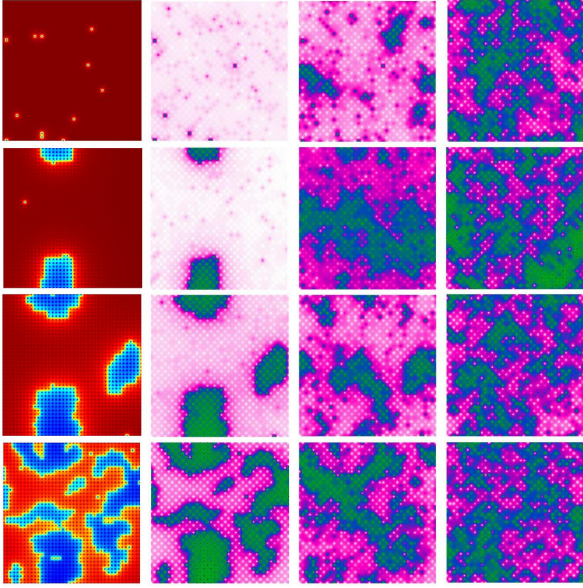


Fig. 3: Colour online: Temperature dependence of short range magnetic correlations. The left column shows ASD configurations, one from each disorder family. $S = 0.98, 0.76, 0.50$ and 0.08 , top to bottom. The 2nd, 3rd and 4th panel along each row is a map of a spin overlap factor, g_i , in a Monte Carlo snapshot. $g_i = \mathbf{S}_0 \cdot \mathbf{S}_i$, where \mathbf{S}_0 is the left lower corner spin in the lattice. The temperatures are $T/t = 0.03, 0.05, 0.07$.

to ‘bulk’ sites is small. The AF coupling between adjoining domains would polarise them antiparallel, and the net moment at $T = 0, h = 0$ would be proportional to the volume difference of up and down domains. We should have $M(T = 0, h = 0) \sim (1 - x) - x = 1 - 2x = S$ so $M^2 = S^2$. Given our S , these are 0.96, 0.58, 0.25, 0.01 in almost perfect correspondence with the $T \rightarrow 0$ values in Fig.2.(a). The elaborate calculation arrives at an obvious answer. The onset temperature for magnetic order seems to be insensitive to the ASD, *i.e.*, the intra-domain order sets in at $T \sim$ the bulk T_c . While our answer for the suppression of magnetisation is $M \sim 1 - 2x$, a 3D calculation, with uncorrelated disorder, had found [15] $M \sim 1 - 1.9x$.

The transport in these background is shown in Fig.2.(b). From weak to intermediate ASD the temperature dependence of $\rho(T)$ remains similar, with a sharp drop near T_c . The only effect of increasing ASD is an increase in residual resistivity. It is as if there is a temperature independent ‘structural’ scattering that gets added to the T dependent magnetic scattering. At large ASD, however, this correspondence breaks down, the $T = 0$ ‘resistivity’ is very large (and grows with growing system size) and $d\rho/dT < 0$. There seems to be a metal-insulator transition between $S = 0.50$ and $S = 0.08$

To create an understanding of this let us focus on $T = 0$, where the magnetic configuration is simple (collinear). The \downarrow spin electrons inhabit the \uparrow core spin domains, and *vice versa*. The conductance arises from the interpenetrating parallel channels for up and down spin elec-

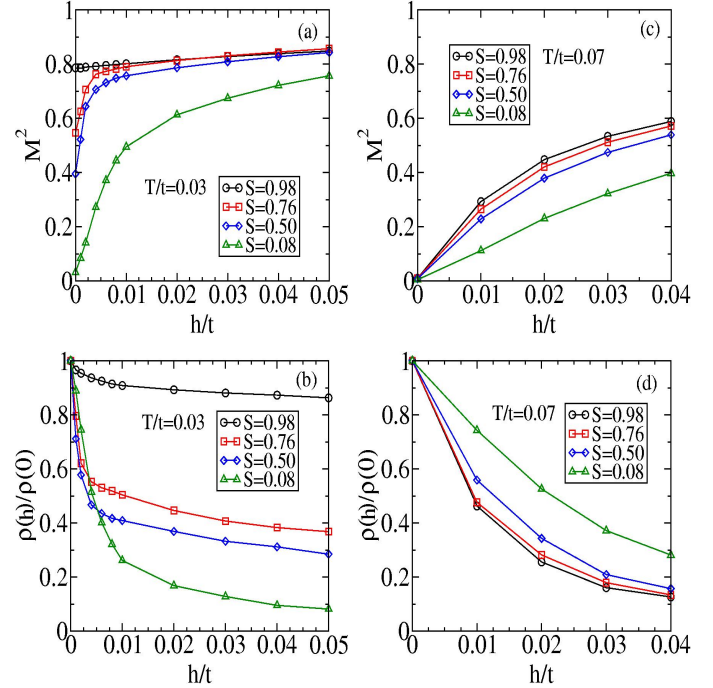


Fig. 4: Colour online: (a)&(c) Field dependence of magnetisation, M^2 , (b)&(d) field dependence of the resistivity, normalised to $h = 0$. The left panels are at ‘low temperature’, $T/t = 0.03$, the right at ‘high temperature’, $T/t = 0.07$.

trons. One could call it “complementary percolation”. Let us identify up electrons with the ‘majority’ phase, and down with the ‘minority’ domains. The net conductivity $\sigma_{tot}(S) = \sigma_{maj}(S) + \sigma_{min}(S)$. While this reduces monotonically with reducing S in our data, Fig.2.(b), the conductivity also depends on p_{corr} . Even at $S = 0$, one could increase σ_{tot} systematically by increasing p_{corr} , *i.e.*, reducing the fragmentation of the conduction paths. Weak localisation effects, *etc.*, in two dimensions could show up at much longer lengthscales, but at a given cutoff size the trend above would survive.

Temperature dependence: The ASD configuration is T independent so the primary sources of T dependence on transport are (i) the weakening of AF locking across the domain boundaries, and (ii) fluctuations about the FM state *within a domain*. The first effect enhances the conductivity, while the second serves as a source of scattering. Their relative importance depends on $\sigma(T = 0)$. For weak disorder (large S) one is far from the percolation threshold and the decrease in σ due to intra-domain magnetic scattering is larger than the enhancement from inter-domain tunneling. However, by the time $S = 0.50$ there is already a weak upturn in ρ as $T \rightarrow 0$, the intra-domain effect is visible, and this becomes the dominant effect as $S \rightarrow 0$.

An analysis of the spatial spin-spin correlations illustrates the AF locking of domains at low temperature and how this weakens with increasing T . The first column in Fig.3 reproduces one set of ASD configurations from

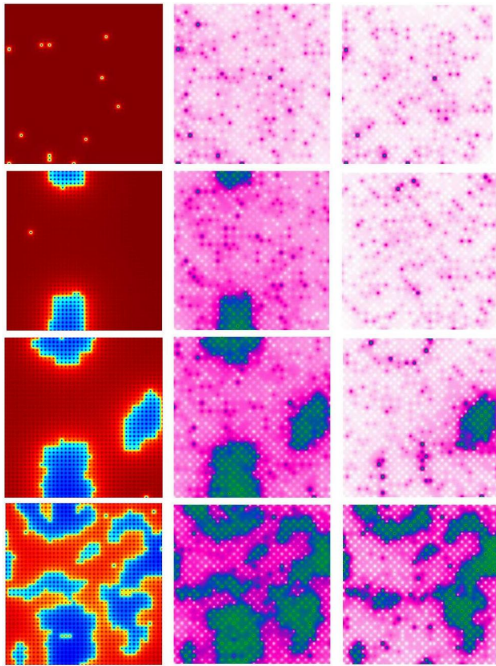


Fig. 5: Colour online: Field dependence of magnetic spatial correlations. We show the usual $g_i = \mathbf{S}_0 \cdot \mathbf{S}_i$, defined earlier. The left column shows the ASD domains, the central column shows g_i at $h/t = 0$, and the right column is for $h/t = 0.001$. The temperature is $T/t = 0.03$.

Fig.1 (the first column). The next three columns show the the magnetic overlap $g_i = \mathbf{S}_0 \cdot \mathbf{S}_i$, where \mathbf{S}_0 is the lower left corner spin in each configuration, for MC snapshots at $T/t = 0.03, 0.05, 0.07$. These pictures would correspond to ‘magnetic domains’ if the patterns survived thermal averaging. The low temperature snapshots correspond closely to the ASD pattern. The antiphase boundary (APB) and the magnetic domain wall (MDW) pattern coincide at $T/t = 0.03$. At $T/t = 0.05$, however, close to the bulk T_c , there is no correlation between the APB and the g_i pattern. There is *significant core spin overlap* across the boundary, and large fluctuation, overall, in spin orientation. This bears out the transport mechanism we suggested in the preceding paragraph.

Field dependence. The field dependence of magnetisation and resistivity is shown in Fig.4., at relatively low temperature, $T/t = 0.03$, in (a)-(b), and high temperature, $T/t = 0.07$, in (c)-(d). Three energies play out when $h \neq 0$: (i) the bulk Zeeman cost of the ‘minority’ domains, $\sim hV_{min}$, where V_{min} is the volume of the minority phase, (ii) the interfacial AF energy, $\sim J_{AF}V(1 - p_{corr})$, where $1 - p_{corr}$ is the fraction of AF bonds on the lattice, and (iii) the *gain in electronic kinetic energy* on removal (or rotation) of MDW’s. (i) and (iii) prefer domain alignment while (ii) prefers to retain domain walls. In a ‘spin only’ model (iii) would be absent. This delocalisation energy gain serves to reduce the field at which domain rotation can occur.

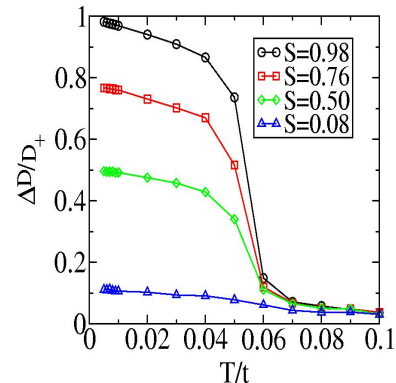


Fig. 6: Colour online: Half-metallicity, estimated as $(D_{\uparrow}(\epsilon_F) - D_{\downarrow}(\epsilon_F)) / (D_{\uparrow}(\epsilon_F) + D_{\downarrow}(\epsilon_F))$, for varying temperature and different degrees of antisite disorder.

At low T , Fig.4.(a)-(b), the ordered samples have a high degree of magnetic order, so the field induced increase in M , and the decrease $\Delta\rho/\rho(0)$, where $\rho(0) = \rho(h = 0)$ and $\Delta\rho = \rho(0) - \rho(h)$, is quite small. The low T low field response is, however, dramatic for low S samples. These samples have $M(h = 0) \sim 0$, and a large $\rho(0)$ due to the fragmented (spin selective) conduction path. A field as small as $h/t \sim 0.001$ leads to $M^2 \sim 0.1$, so $M \sim 0.3$. The corresponding impact on spin correlations is shown in the lowest row in Fig.5, where the MDW pattern is strongly affected by h . While the domain rotation effect is visible both for $S = 0.50$ and $S = 0.08$, the less disordered sample had a larger conductivity at $h = 0$ so the fractional change is much larger for $S = 0.08$.

At high temperature, Fig.4.(c)-(d), the domains cease to exist and conductance gain from domain rotation is irrelevant. In the large S samples there are few AF links so the applied field just suppresses the magnetic fluctuations leading to large $\Delta\rho/\rho(0)$. In the most disordered samples there are $(1 - p_{corr})/2 \sim 7\%$ of AF bonds. Although there are no domains, these act as a source of scattering. The gain in conductivity is slower in the disordered samples compared to the more ordered ones.

Half metallicity. These systems are unusual because at $T = 0$ within each domain the conduction electron has only one spin polarisation but averaged over the system both \uparrow and \downarrow electrons have density of states at ϵ_F . A local probe, with probe area $< \xi^2$, will allow only spin polarised tunneling, while a probe averaging over domains will see both $D_{\uparrow}(\epsilon_F)$ and $D_{\downarrow}(\epsilon_F)$. Fig.6 shows $(D_{\uparrow}(\epsilon_F) - D_{\downarrow}(\epsilon_F)) / (D_{\uparrow}(\epsilon_F) + D_{\downarrow}(\epsilon_F))$ as a measure of half-metallicity. It is unity only in the absence of ASD and at $T = 0$, and in general has a behaviour that broadly mimics the behaviour of the core spin magnetisation, Fig.2.(a).

Discussion. – There are two issues we want to touch upon, to relate our work to real double perovskites. (a). The role of dimensionality: it is well known that localisation effects are stronger in 2D compared to 3D, so we

ran this entire calculation on a 12^3 system to check out the trends in transport. In particular we confirmed that there indeed is a sharp rise in the residual resistivity (although possibly no insulating phase) with increasing ASD. The low temperature upturn in $\rho(T)$ is present, but weaker, even in 3D. (b). Role of grain boundaries: in the absence of a chemical characterisation of the grain boundary material, and an electronic model for the GB, it is hard to construct a comprehensive theory. However, since grain size, $l_G \gg \xi$, it should be possible to study the role of APB's and MDW's via non contact probes that focus on a single grain.

Conclusion. – We have studied a double perovskite model on antisite disordered backgrounds with a high degree of short range correlation. In this situation, the antiphase boundaries coincide with the $T = 0$ magnetic domain walls. Growing ASD reduces the low field magnetization, destroys the half-metallicity, and leads to a low temperature metal-insulator transition. While these are disadvantages, we also note that the ferromagnetic T_c is only weakly affected by moderate ASD and the low field magnetoresistance is dramatically enhanced by disorder. Our real space results allow an interpretation of these in terms of the domain pattern, the effective exchange, and the short range magnetic correlations. They are also consistent with explicit spatial imagery from recent experiments. The ‘intra-grain’ effects highlighted here would be directly relevant to single crystals, and define the starting point for a transport theory of the polycrystalline double perovskites.

Acknowledgements: We acknowledge use of the Beowulf Cluster at HRI and discussions with G. V. Pai, P. Sanyal, D. D. Sarma, and R. Tiwari. PM acknowledges support from a DAE-SRC Outstanding Research Investigator Award, and the DST India through the Indo-EU ATHENA project.

REFERENCES

- [1] For reviews, see D. D. Sarma, *Current Op. Solid St. Mat. Sci.*, **5**, 261 (2001), D. Serrate, J. M. de Teresa and M. R. Ibarra, *J. Phys. Cond. Matt.* **19**, 023201 (2007).
- [2] K.-I. Kobayashi, T. Kimura, H. Sawada, K. Terakura and Y. Tokura, *Nature* **395**, 677 (1998).
- [3] Y. Tomioka, T. Okuda, Y. Okimoto, R. Kumai, K.-I. Kobayashi, and Y. Tokura, *Phys. Rev. B* **61**, 422 (2000).
- [4] K.-I. Kobayashi, T. Okuda, Y. Tomioka, T. Kimura and Y. Tokura, *Jl Magn and Magn Matls*, 218, 17 (2000).
- [5] H. Das, U. V. Waghmare, T. Saha-Dasgupta, and D. D. Sarma, *Phys. Rev. Lett.* **100**, 186402 (2008).
- [6] D. D. Sarma, P. Mahadevan, T. Saha-Dasgupta, S. Ray, and A. Kumar, *Phys. Rev. Lett.* **85**, 2549 (2000).
- [7] A. Chattopadhyay and A. J. Millis, *Phys. Rev. B* **64**, 024424 (2001).
- [8] P. Sanyal and P. Majumdar, *Phys. Rev. B* **80**, 054411 (2009).
- [9] M. Garcia-Hernandez, J. L. Martinez, M. J. Martinez-Lope, M. T. Casais, and J. A. Alonso, *Phys. Rev. Lett.* **86**, 2443 (2001).
- [10] Y. H. Huang, M. Karppinen, H. Yamauchi, and J. B. Goodenough, *Phys. Rev. B* **73**, 104408 (2006).
- [11] Y. H. Huang, H. Yamauchi, and M. Karppinen, *Phys. Rev. B* **74**, 174418 (2006).
- [12] J. Navarro, L. Balcells, F. Sandiumenge, M. Bibes, A. Roig, B. Martnez and J. Fontcuberta, *J. Phys. Cond. Matt* **13**, 8481 (2001).
- [13] J. Navarro, J. Nogues, J. S. Munoz, and J. Fontcuberta, *Phys. Rev. B* **67**, 174416 (2003).
- [14] D. D. Sarma, S. Ray, K. Tanaka, M. Kobayashi, A. Fujimori, P. Sanyal, H. R. Krishnamurthy and C. Dasgupta, *Phys. Rev. Lett.*, **98**, 157205 (2007).
- [15] J. L. Alonso, L. A. Fernandez, F. Guinea, F. Lesmes, and V. Martin-Mayor, *Phys. Rev. B* **67**, 214423 (2003).
- [16] C. Frontera and J. Fontcuberta, *Phys. Rev. B* **69**, 014406 (2004).
- [17] T. Asaka, X. Z. Yu, Y. Tomioka, Y. Kaneko, T. Nagai, K. Kimoto, K. Ishizuka, Y. Tokura, and Y. Matsui, *Phys Rev B* **75**, 184440 (2007).
- [18] C. Meneghini, Sugata Ray, F. Liscio, F. Bardelli, S. Mobilio, and D. D. Sarma, *Phys. Rev. Lett.* **103**, 046403 (2009).
- [19] D. Niebieskikwiat, F. Prado, A. Caneiro, and R. D. Sanchez, *Phys. Rev. B* **70**, 132412 (2004).
- [20] P. Sanyal, S. Tarat and P. Majumdar, *Eur. Phys. J. B* **65**, 39 (2008).
- [21] In SFMO ($\epsilon_B - J/2$) - $\epsilon_{B'}$ $\sim 5t$, and we have checked that this B, B' energy mismatch mainly serves to enhance the resistivity without affecting the trends we observe.
- [22] S. Kumar and P. Majumdar, *Eur. Phys. J. B* **50**, 571-579 (2006).
- [23] S. Kumar and P. Majumdar, *Eur. Phys. J. B* **46**, 237 (2005).